

# Josephson junctions and superconducting quantum interference devices made by local oxidation of niobium ultrathin films

V. Bouchiat<sup>a)</sup> and M. Faucher

GPEC, UMR CNRS 6631, Université de la Méditerranée, Case 901, 13288 Marseille, France

C. Thirion and W. Wernsdorfer

Laboratoire Louis Néel, UPR CNRS 5051, BP 166, 38042 Grenoble, France

T. Fournier and B. Pannetier

CRTBT, UPR CNRS 5001, BP 166, 38042 Grenoble, France

(Received 9 November 2000; accepted for publication 8 May 2001)

We present a method for fabricating Josephson junctions and superconducting quantum interference devices (SQUIDs) which is based on the local anodization of niobium strip lines 3–6.5 nm thick under the voltage-biased tip of an atomic force microscope. Microbridge junctions and SQUID loops are obtained either by partial or total oxidation of the niobium layer. Two types of weak link geometries are fabricated: lateral constriction (Dayem bridges) and variable thickness bridges. SQUIDs based on both geometries show a modulation of the maximum Josephson current with a magnetic flux periodic with respect to the superconducting flux quantum  $h/2e$ . They persist up to 4 K. The modulation shape and depth of SQUIDs based on variable thickness bridges indicate that the weak link size becomes comparable to the superconducting film coherence length  $\xi$  which is of the order of 10 nm. © 2001 American Institute of Physics. [DOI: 10.1063/1.1382626]

Nanolithography using scanning probe microscopes (SPMs) offers powerful methods<sup>1</sup> for patterning surfaces with a resolution beyond the range of conventional lithographies based on resist exposures. During the last decade, these techniques have brought some important features to device fabrication, such as easy alignment and *in situ* control of the device electrical characteristics during its fabrication.<sup>2</sup> Furthermore, local probe techniques, based on near field interactions, show a greatly reduced proximity effect<sup>3</sup> which limits resolution in e-beam lithography. On the one hand, lithography using UHV-scanning tunneling microscopes (STMs) leads to ultimate resolution (i.e., at the atomic scale),<sup>4,5</sup> but the building of structures with a permanent and stable electrical connection<sup>6</sup> has not been completely achieved. On the other hand, non-UHV-SPM lithography techniques are mainly based on the atomic force microscope (AFM). These latter techniques, based either on tip indentation<sup>7–9</sup> or on a voltage biased tip,<sup>10–19</sup> retain nanometer scale resolution and show better versatility. Among these resistless AFM lithographies, local anodization of the surface of a semiconductor<sup>11,12</sup> or of non-noble metals<sup>13–15</sup> by the biased tip of an AFM is a versatile method by which to make nanoscale quantum devices. Quantum point contacts,<sup>11,13</sup> nanowires,<sup>12</sup> single electron devices,<sup>14</sup> superconducting devices<sup>16</sup> as well as other nanoscale devices involving nanotubes<sup>17</sup> or clusters<sup>18</sup> have been obtained.

In order to fabricate the structure in a single step, the film thickness must be less than the typical depth of oxidized metal (i.e., 10 nm), thus allowing direct writing of fully insulating regions. Such a process can be controlled well and is sufficiently reproducible to control the oxide linewidth to values defining either a complete electrical separation or, for

a single line drawn at high speed and low voltage, a metal/insulator/metal tunnel barrier with low transparency.<sup>15</sup> The intrinsic ultrasmall capacitance of such tunnel junctions has been exploited to produce single electron devices operating at room temperature.<sup>14</sup>

In this letter, we present an application of this anodization technique for fabricating superconducting nanostructures using high quality ultrathin niobium films. As an initial demonstration of potential applications for mesoscopic superconductivity, we have made and tested at low temperature a series of dc-superconducting quantum interference devices (SQUIDs) based on microbridge technology with various geometries.

A single crystal sapphire wafer was chosen as the substrate for ultrathin film growth. It has a  $\bar{1}102$  orientation with an off-axis miscut as low as possible (about  $10^{-3}$  rad). After thermal treatment at 1100 °C for 1 h in air,<sup>19</sup> the sapphire surface is reconstructed such that 0.3–0.8  $\mu\text{m}$  wide, atomically flat terraces separated by 0.3 nm high steps are observed [visible in Fig. 1(b)]. A niobium layer with thickness of either 3 or 6.5 nm is then epitaxially grown using an electron gun evaporator in UHV conditions. The sapphire substrate was *in situ* cleaned by Ar ion milling and heated at 550 °C during Nb deposition.<sup>20</sup> In order to prevent rapid aging of the film, a 2 nm thick silicon layer is deposited on top at room temperature in the same vacuum.<sup>21</sup> As expected, the films show superconducting properties slightly depressed with respect to the bulk:<sup>20</sup> the critical temperatures of the bare films are, respectively, 5 and 6.6 K, while their residual resistivity ratios ( $T=300/4.2$  K) are 1.5 and 2.2.<sup>22</sup>

Before proceeding to the AFM lithography, a prefabrication step is performed in order to define the electrical connections. The film is patterned using standard UV lithography techniques and is dry etched in a SF<sub>6</sub> plasma to define

<sup>a)</sup>Author to whom correspondence should be addressed; electronic mail: bouchiat@gpec.univ-mrs.fr

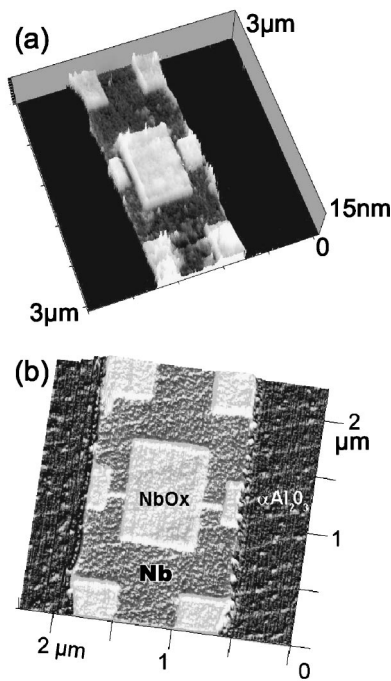


FIG. 1. AFM micrographs of 6.5 nm thick niobium strip lines on which SQUIDs have been made by AFM-controlled anodization. The brightest regions are the patterned niobium oxide protrusions. (a) The microbridges on each side of the loop consist of 50 nm wide, 400 nm long lateral constrictions, reminiscent of “Dayem”-type bridges. (b) The bridges have a variable thickness made by oxide lines that locally reduce the niobium layer. 0.3 nm high atomic steps and their replicas can be seen on the bare sapphire substrate (dark lateral areas) as well as on the top of both the raw and patterned surfaces, thus showing the structural quality of the deposited and oxidized layers.

1–3  $\mu\text{m}$  wide strip lines. Their electrical resistance is of the order of 60  $\Omega/\text{sq}$  for the 6.5 nm thick Nb layer. The wafer is then diced and AFM lithography is performed using the contact mode with a commercial PtIr-covered tip. A negative voltage ranging between 4 and 14 V is applied to the tip with respect to the grounded film. This voltage depends on both the desired oxide depth and the tip quality. We have found that the silicon top layer does not affect the oxidation of the Nb layer underneath.

Large insulating areas are obtained by scanning the biased tip in lines laterally separated by 10–40 nm. Since tunneling barriers obtained by a single oxide line diffusing through the whole layer thickness are still too thick to produce a measurable Josephson tunneling current,<sup>14</sup> our Josephson junctions are based on superconducting weak links.<sup>23</sup> The idea is simply to pattern two local constrictions (microbridges) on the strip line separated by the insulating loop center. Figure 1 shows AFM images of two types of SQUIDs chosen from the  $\sim 40$  devices fabricated. Microbridges can be clearly seen on both sides of the strip line: oxidized areas which are thicker than the bare niobium film appear bright in the AFM micrographs. Two types of microbridge geometry have been successfully tested. First we have fabricated SQUIDs with so-called “Dayem” bridges.<sup>24</sup> These bridges consist of superconducting lateral constrictions of between 30 and 100 nm in width and 200–1000 nm in length [Fig. 1(a)]. Their resistance in the normal state is estimated to be several hundred ohms.

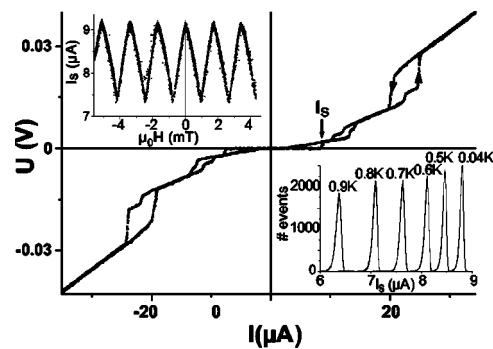


FIG. 2. Voltage–current characteristics measured at 40 mK of the Dayem SQUID shown in Fig. 1(a). The switching current  $I_s$  is defined as the maximum observed Josephson current. The hysteresis observed between ramp up and ramp down is due to Joule heating in the strip line. Top inset: Magnetic field dependence of  $I_s$ , measured at 0.5 K. Bottom inset: Temperature dependence of the  $I_s$  normalized histograms taken at 10 kHz.

Figure 2 presents the electrical characterization at low temperature of the sample imaged in Fig. 1(a). Switching currents  $I_s$  (see the arrow in Fig. 2) are defined as maximum dc-Josephson currents measured before reaching the nonzero-voltage dissipative regime. Nonlinearities at finite voltage come from heat induced transitions: their positions depend on the current sweeping frequency.

In the AFM-made Dayem-like SQUIDs presented in Fig. 1(a), the modulation of  $I_s$  with magnetic field exhibits a sharp symmetric sawtooth shape with modulation depth  $\Delta I_s/I_s$  of 12%–18%, where  $\Delta I_s$  is the peak-to-peak modulation depth. The period was reproducibly found to be around 2 mT (Fig. 2, top inset), a value in good agreement with the predicted period of  $\phi_0/S$ , where  $S$  is the loop area ( $\sim 1 \mu\text{m}^2$ ) and  $\phi_0$  the superconducting flux quantum  $h/2e$ . The linear dependence of  $I_s(\Phi)$ , as well as the reduced modulation depth, could suggest that the loop screening currents are strong enough to partially wash out the interference pattern. However the calculated loop inductance  $L$  of our device ( $2pH$ ) leads to a reduced screening factor  $LI_s/\Phi_0=0.003$ , negligible compared to 1. Therefore the loop inductance is too small to account for the interference pattern observed. The device is thus dominated by the kinetic inductance of the weak links. This is a common feature of SQUIDs based on microbridges that have sizes much larger than the superconducting film coherence length  $\xi$ .<sup>23</sup>

Histograms of  $I_s$  exhibit a distribution shape typically found in Josephson junctions<sup>25</sup> from which we derive a residual noise of  $1.5 \times 10^{-4} \phi_0/\text{Hz}^{1/2}$  at 40 mK. This first series of samples has roughly comparable behavior to those similar in design, based on thicker Nb Dayem bridges and fabricated by electron beam lithography (EBL).<sup>26</sup>

In order to reduce further the weak-link size, we have tried another design. Starting from a SQUID fabricated using the method described above, a 15 nm wide single oxide line partially oxidizing the niobium layer is drawn across both Dayem microbridges [see Figs. 1(b) and 3(b)]. This kind of buried nanostructure belongs to another family of weak links, variable thickness bridges.<sup>23</sup> The resulting field modulation of  $I_s$  obtained for these devices (Fig. 3, bottom) follows a pattern which differs from previously presented Dayem SQUIDs. In every device tested based on this second type of weak link, the modulation depth  $\Delta I_s/I_s$  is enhanced

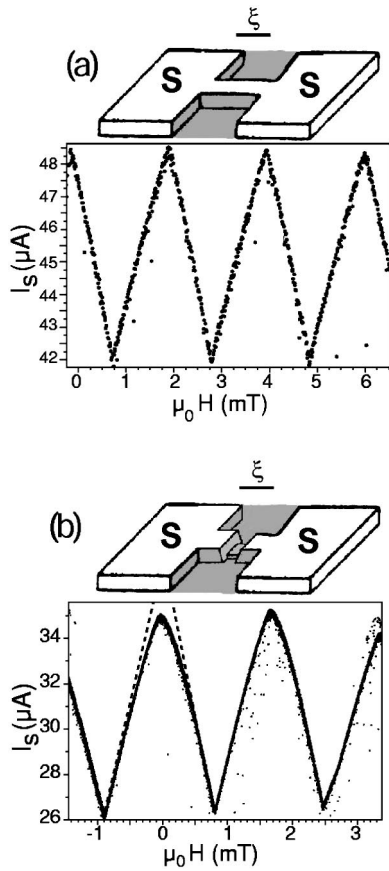


FIG. 3. Schematic diagrams describing the two kinds of microbridges (the gray area corresponds to grown oxide) and measured flux modulation of the switching current ( $T=40$  mK) for SQUIDs based on each geometry. (a) For SQUIDs with  $0.3 \mu\text{m}$  long Dayem-like bridges, perfect sawtooth modulation is obtained, since the bridges have widths and lengths larger than the superconducting coherence length  $\xi$ . (b) For SQUIDs with variable thickness bridges, the magnetic field dependence of  $I_s$  shows deviation from linear behavior (dotted line) while the modulation depth is increased with respect to curve (a). These features are signatures of Josephson junctions of dimensions shorter than  $\xi$ .

by roughly a factor of 2 with respect to that of previous devices. Furthermore, clear deviation from the linear dependence of  $I_s(\phi)$  is observed near the current maxima [Fig. 3(b)]. As pointed out in Ref. 23, these two phenomena are related to the smaller size of the weak links whose characteristic dimensions become of the order of the superconducting film coherence length  $\xi$  (estimated to be around 10 nm).

The effective cross section of the microbridges for that geometry is not known exactly but is estimated to be around 50 nm wide and 3 nm thick by measuring the niobium oxide height. Depending on the film thickness and quality, the critical current density in our junctions varied from 0.3 to 8  $\text{MA}/\text{cm}^2$ .

We have checked that these devices have sufficiently high critical magnetic field in the in-plane direction to allow local magnetic flux detection. Indeed, EBL-made Dayem SQUIDs have already enabled powerful magnetometry techniques in nanomagnetism,<sup>27</sup> and have led to measurements of

magnetization reversal in nanoscale magnetic particles. AFM-made devices should offer new features such as the fabrication at a chosen position, allowing optimized coupling to magnetic signals, and increased intrinsic sensitivity. In the case of small magnetic clusters which are placed very close to the microbridge junctions, we also expect an improvement of one to two orders of magnitude due to reduction of the microbridge size. It might allow us to detect spin flips of about 100 magnetic moments.

The authors are indebted to G. Battuz and A. Hadj-Azzem for substrate preparation and to A. Bychkov for ultrathin film characterization. V. Safarov, F. Salvan, and K. Hasselbach are gratefully acknowledged for help and discussions.

<sup>1</sup>For a review on early developments in STM lithography, see, for example, R. Wiesendanger, *Appl. Surf. Sci.* **54**, 271 (1992).  
<sup>2</sup>E. S. Snow and P. M. Campbell, *Science* **270**, 1639 (1995).  
<sup>3</sup>K. Wilder, B. Singh, D. F. Kyser, and C. F. Quate, *J. Vac. Sci. Technol. B* **16**, 3864 (1998); M. Ishibashi, S. Heike, H. Kajiyama, Y. Wada, and T. Hashizume, *Jpn. J. Appl. Phys., Part 1* **37**, 1565 (1998).  
<sup>4</sup>D. M. Eigler and K. L. Schweizer, *Nature (London)* **34**, 524 (1990).  
<sup>5</sup>H. C. Manoharan, C. P. Lutz, and D. M. Eigler, *Nature (London)* **403**, 512 (2000).  
<sup>6</sup>G. Palasantzas, B. Ilge, S. Rogge, and L. J. Geerligs, *Microelectron. Eng.* **46**, 133 (1999).  
<sup>7</sup>L. L. Sohn and R. L. Willet, *Appl. Phys. Lett.* **67**, 1552 (1995).  
<sup>8</sup>V. Bouchiat and D. Estève, *Appl. Phys. Lett.* **69**, 3098 (1996).  
<sup>9</sup>B. Irmer, R. H. Blick, F. Simmel, W. Gödel, H. Lorenz, and J. P. Kotthaus, *Appl. Phys. Lett.* **73**, 2051 (1998).  
<sup>10</sup>J. A. Dagata, J. Schneir, H. H. Harary, C. J. Evans, M. T. Postek, and J. Bennett, *Appl. Phys. Lett.* **56**, 2001 (1990).  
<sup>11</sup>R. Held, T. Heinzel, P. Studerus, K. Ensslin, and M. Holland, *Appl. Phys. Lett.* **71**, 2689 (1997); R. Held, T. Vancura, T. Heinzel, K. Ensslin, M. Holland, and W. Wegscheider, *ibid.* **73**, 262 (1998).  
<sup>12</sup>E. S. Snow and P. M. Campbell, *Appl. Phys. Lett.* **64**, 1932 (1994).  
<sup>13</sup>E. S. Snow, D. Park, and P. M. Campbell, *Appl. Phys. Lett.* **69**, 269 (1996).  
<sup>14</sup>K. Matsumoto, M. Ishii, K. Segawa, Y. Oka, B. J. Vartanian, and J. S. Harris, *Appl. Phys. Lett.* **68**, 34 (1996); see also K. Matsumoto, *ibid.* **72**, 1893 (1998); K. Matsumoto, Y. Gotoh, T. Maeda, J. Dagata, and J. Harris, *ibid.* **76**, 239 (2000).  
<sup>15</sup>B. Irmer, M. Kehrle, H. Lorentz, and J. P. Kotthaus, *Appl. Phys. Lett.* **71**, 1733 (1997).  
<sup>16</sup>I. Song, B. M. Kim, and G. Park, *Appl. Phys. Lett.* **76**, 601 (2000).  
<sup>17</sup>P. Avouris, T. Hertel, R. Martel, T. Schmidt, H. R. Shea, and R. E. Walkup, *Appl. Surf. Sci.* **141**, 201 (1999).  
<sup>18</sup>R. J. M. Vullers, M. Ahlskog, M. Cannaearts, and C. van Haesendonck, *Appl. Phys. Lett.* **76**, 1947 (2000).  
<sup>19</sup>K. Matsumoto, Y. Gotoh, J. Shirakashi, T. Maeda, and J. S. Harris, *Proceedings of IEDM '97* (IEEE, Piscataway, NJ, 1997), p. 155.  
<sup>20</sup>S. I. Park and T. H. Geballe, *Physica B* **135**, 108 (1985).  
<sup>21</sup>J. M. Graybeal and M. R. Beasley, *Phys. Rev. B* **29**, 4167 (1984).  
<sup>22</sup>K. Yoshii, H. Yamamoto, K. Saiki, and A. Koma, *Phys. Rev. B* **52**, 13570 (1995).  
<sup>23</sup>K. K. Likharev, *Rev. Mod. Phys.* **51**, 101 (1979).  
<sup>24</sup>P. W. Anderson and A. H. Dayem, *Phys. Rev. Lett.* **13**, 195 (1964); A. H. Dayem, *Appl. Phys. Lett.* **9**, 47 (1966).  
<sup>25</sup>T. A. Fulton and L. N. Dunkleberger, *Phys. Rev. B* **9**, 4760 (1974).  
<sup>26</sup>C. Chapelier, M. El-Khatib, P. Perrier, A. Benoit, and D. Mailly, *Proceedings of the 4th International Conference, SQUID'91* (Springer, Berlin, 1991).  
<sup>27</sup>W. Wernsdorfer, E. B. Orozco, K. Hasselbach, A. Benoit, B. Barbara, N. Demoncey, A. Loiseau, H. Pascard, and D. Mailly, *Phys. Rev. Lett.* **78**, 1791 (1997).